CrossMark

INVITED REVIEW

Stabilizing and scaling up carbon-based perovskite solar cells

Haining Chen[a)]
School of Materials Science and Engineering, Beihang University, Beijing 100191, People's Republic of China
Shihe Yang[b)]
Department of Chemistry, The Hong Kong University of Science and Technology, Kowloon, Hong Kong, China

(Received 25 April 2017; accepted 30 June 2017)

Organometal trihalide perovskite solar cells (PSCs) have sparked a frantic excitement in the scientific community because they can achieve high power conversion efficiencies (PCEs) even when fabricated by low-cost solution-processing technologies. However, the poor stability of PSCs has seriously hindered their commercialization. Among various kinds of PSCs, carbon-based PSCs without hole transport materials (C-PSCs) seem to be the most promising for addressing the stability issue because carbon materials are stable, inert to ion migration, and inherently water-resistant. Concurrent with the steady rise in PCE of C-PSCs, great progresses have also been attained on the device stability and scaling-up fabrication of C-PSCs, which have well signified the possible commercialization of PSCs in the near future. In this review, we will summarize these progresses with a view of exposing the promising prospect. We start by collating recent stability testing results of C-PSCs with reference to those of HTM-PSCs. Then, we update the research status on large-scale C-PSCs and their associated scalable fabrication technologies. Finally, we identify main issues to be addressed alongside future research directions.

I. INTRODUCTION

Organometal trihalide perovskite solar cells (PSCs) have attracted wide attention because such a solution process-based photovoltaic device has obtained comparable power conversion efficiencies (PCEs) (over 22%) with traditional commercial solar cells in a short time span of its development.[1–12] The special and advantageous optoelectronic properties of the hybrid materials (ABX_3: A = CH_3NH_3, $HC(NH_2)_2$, Cs; B = Pb, Sn; X = Cl, Br, I) that account for the rapid growth in PCE,[7,13] include high mobility,[14–17] long balanced carrier diffusion length,[15,16,18,19] and low exciton binding energy.[20]

Despite the high PCEs and the solution-based processes advantageous in commercializing PSCs, the poor device stability significantly hampered the application. The instability problem is caused not only by the perovskite itself but also by the conventional organic hole transport material (HTM), such as spiro-OMeTAD, PTAA, P3HT. Organic HTM layers are usually open and susceptible to migration of halide ions and metal ions (from the metal electrode), which inevitably result in device degradation.[21–27] Besides, most of these organic HTMs are expensive and operationally unstable (usually require inert atmosphere). Fortunately, researchers have proved that perovskites (e.g., $CH_3NH_3PbI_3$) could serve as both a light harvester and a hole transporter,[18,19,28,29] thus facilitating HTM-free PSCs.[29–34]

So far, several types of HTM-free PSCs have been developed with using Au,[28,35] Ni,[36] or carbon[29,37–39] as hole extraction electrodes. Due to the obvious advantageous properties of carbon electrodes, including low cost, high stability, inertia to ion migration, and high water resistance, carbon-based HTM-free PSCs (C-PSCs) have exhibited significantly higher stability than HTM-PSCs.[34,40] After the initial report in 2013, the PCE of C-PSCs has increased gradually from 6.64% to 15.9%,[29,30,41–47] which makes it among the most promising PSCs devices for commercialization. As a result, several research groups and companies have worked together to promote the commercialization of C-PSCs, and some scalable techniques have been exploited to fabricate large-scale devices.

Since great progresses have been achieved on the device stability and the scaling up of C-PSCs, herein, we aim to document these progresses to illustrate the promising prospect for their commercialization. Firstly, we will catalog and discuss the recent stability results of C-PSCs with an emphasis on a clear comparison with those of HTM-PSCs. Then, the research status on the large-scale C-PSCs will be appraised, including device structures and scalable techniques. Finally, main issues and future research directions will be addressed.

Contributing Editor: Gary L. Messing
Address all correspondence to these authors.
[a)]e-mail: chenhaining@buaa.edu.cn
[b)]e-mail: chsyang@ust.hk
DOI: 10.1557/jmr.2017.294

 © Materials Research Society 2017

https://doi.org/10.1557/jmr.2017.294 Published online by Cambridge University Press

II. DEVICE STRUCTURES AND WORKING PRINCIPLES OF C-PSCS

As illustrated in Fig. 1(a), C-PSCs usually consist of FTO/TiO_2 dense layer/TiO_2 mesoporous layer/perovskite/carbon. The general working principles of C-PSCs are illustrated in Fig. 1(b). After light illumination, electrons and holes are produced in the conduction band (CB) and valence band (VB) of the perovskite, respectively. The photogenerated electrons produced in the CB of the perovskite are subsequently injected into the CB of TiO_2 and transported to the FTO substrate, while the photogenerated holes in the VB of the perovskite are extracted by carbon electrodes. The initial work was reported by Ku et al. in 2013, which achieved a PCE of about 6.6% [Fig. 1(c)].[29] After one year, they further push the PCE to 12.8%.[30] In 2016, Chen et al. boosted the PCE to 14.38%.[48] Very recently, Zhang et al. have promoted the PCE to 15.9%.[43]

According to the device structure and fabrication procedure, C-PSCs could be divided into three types: meso C-PSCs, embedment C-PSCs, and paintable C-PSCs (Fig. 1).[41] Meso PSCs, developed by Ku et al [Fig. 1(d)],[29] comprise of a multi-layer mesoporous structure, followed by the infiltration of a perovskite solution.[29,49] Embedment C-PSCs were explored by Wei et al.,[37] in which the carbon electrode was deposited onto a predeposited PbI_2 layer, followed by postconverting PbI_2 to $MAPbI_3$. Paintable C-PSCs were originated from the clamping concept reported in the initial paper on embedment C-PSCs,[32,37,40] in which the carbon electrode in paste or paint form is deposited on a perovskite layer using either a painting process or a doctor blade technique, at low temperature. Though all these C-PSCs operate via similar charge transport principles, their different device structures and fabrication processes have led to significantly different photovoltaic performance.

III. THE HIGH STABILITY OF C-PSCS

The first reported C-PSCs are the well-known meso C-PSCs developed by Ku et al.,[29] which have a typical multi-layer mesoporous structure, including TiO_2, ZrO_2, and porous carbon layers, serving as the electron transporting layer, insulating layer, and hole extraction layer, respectively. The TiO_2 and ZrO_2 mesoporous layers in these meso C-PSCs were fabricated from nanoparticles, while the carbon mesoporous layer (at least several micrometers thick) was carbon black and layered graphite. Finally, a perovskite precursor solution was infiltrated into the multi-layer mesoporous structure by applying the precursor solution dropwise to the surface to obtain the meso C-PSCs.

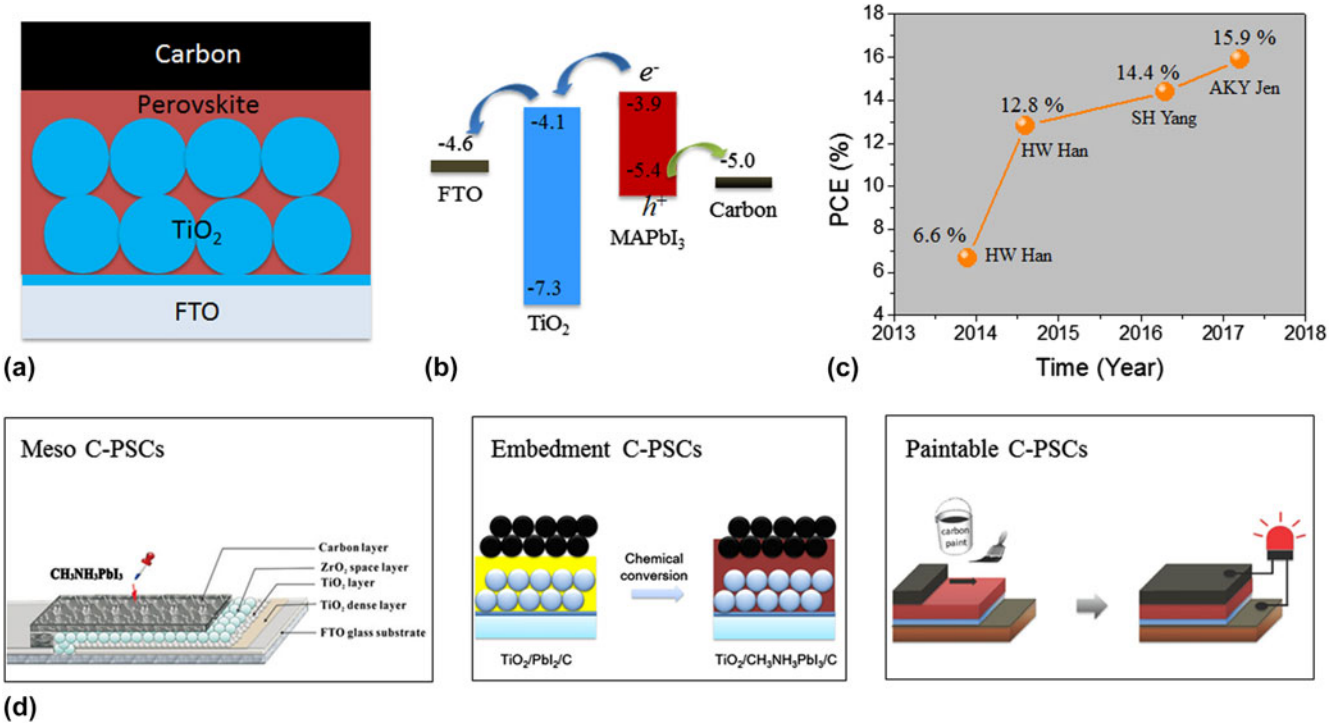


FIG. 1. Device structure, working principle and efficiency evolution of C-PSCs. (a) Structure of C-PSCs, (b) schematic energy level diagram and charge transfer behavior in C-PSCs, (c) reported efficiency evolution of C-PSCs, and (d) structure and fabrication processes of three types of C-PSCs. Reprinted with permission from Refs. 29, 41, and 46. Copyright 2013, Nature Publishing Group. Copyright 2017, Wiley. Copyright 2016, Wiley.

https://doi.org/10.1557/jmr.2017.294 Published online by Cambridge University Press

The ultra-high stability is the obvious advantage of meso C-PSCs. The initial meso C-PSCs fabricated from the $MAPbI_3$ perovskite solution containing PbI_2 and MAI exhibited almost no performance decay after storage in dark (dry air and room temperature) for 840 h.[29] by introducing $HOOC(CH_2)_4NH_3I$ (5-AVAI) into the precursor solution to partially replace MAI, the obtained mixed perovskite of $(5\text{-AVA})_x(MA)_{1-x}PbI_3$ not only significantly improved pore filling capacity to promote the PCE to 12.8% but also greatly improved the device stability.[29,50] Both the large and small nonencapsulated devices retained their initial photovoltaic performance after light soaking in an air atmosphere for over 1000 h [Fig. 2(a)].

Such a high stability of the C-PSCs foreshadows the opportunity for their commercialization. To verify the commercializing feasibility and potential, Li et al. have comprehensively investigated the stability of such devices by means of both practical and accelerated tests.[51] During outdoor aging in Jeddah, Saudi Arabia, the device performed adequately after 7 days [Fig. 2(b)]. Following storage in a dark, normal oven under ambient air at 80–85 °C for 90 days, no obvious PCE decay was observed [Fig. 2(c)]. More promisingly, a systematic stability evaluation conducted by Baranwal et al. showed that almost no PCE degradation was observed for encapsulated meso C-PSCs in ambient air at 100 C [Fig. 2(d)].[52] These promising results on stability confirmed that meso C-PSCs could provide a promising path toward realizing efficient and stable PSCs.

The above-mentioned device stability is considerably higher than those of HTM-PSCs, which is the most advantageous feature of C-PSCs. To highlight this advantage, we have collected some representative stability testing results on HTM-PSCs and C-PSCs for a clear comparison (Table I). Obviously, higher photo stability and thermal stability were demonstrated of C-PSCs, especially under harsh testing conditions (AM1.5 G, 100 mW/cm^2, and 85–100 °C).[30,51–53] Moreover, promising outdoor stability results have also been achieved (under hot and high humid climate at Jeddah, Saudi Arabia).[51] However, for HTM-PSCs, most of the stability

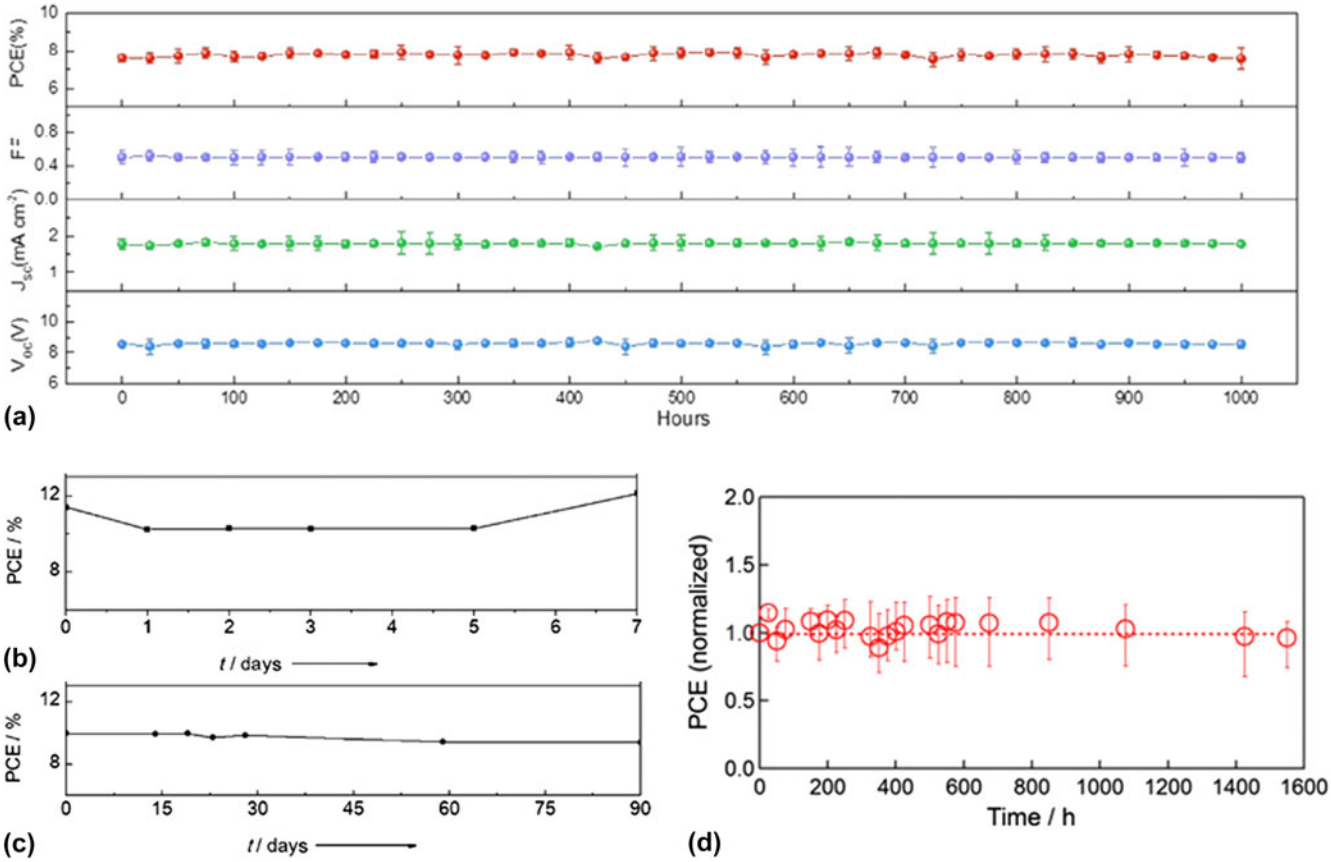


FIG. 2. Stability testing results of C-PSCs. (a) Photovoltaic change with time under light soaking (AM 1.5, 100 mW/cm^2) in ambient air. Reprinted with permission from Ref. 53. Copyright 2017, Wiley. (b) PCE variation of encapsulated meso C-PSCs during outdoor aging in Jeddah, Saudi Arabia and (c) PCE variation of encapsulated meso C-PSCs in ambient air at 80–85 °C. Reprinted with permission from Ref. 51. Copyright 2015, Wiley. (d) Normalized PCE variation of encapsulated meso C-PSCs in ambient air at 100 °C. Reprinted with permission from Ref. 52. Copyright 2016, Wiley.

https://doi.org/10.1557/jmr.2017.294 Published online by Cambridge University Press

testing conditions were modified, and promising thermal stability has been rarely reported. For example, several researches have used a filter to remove the UV light from the incident illumination by using a glass filter or polymer coating.[50,54,55] Some other researches have conducted the stability measurement in N_2 atmosphere, which is far from ambient atmosphere.[55,56] The exploitation of two dimensional (2D) perovskite and all inorganic collection layers seem to have improved the device stability of HTM-PSCs, but the PCE was well suppressed.[57] Moreover, thermal stability in ambient atmosphere has not been reported yet, indicating that the road to commercializing HTM-PSCs is far from that of C-PSCs.

In parallel, embedment C-PSCs and paintable C-PSCs have also demonstrated considerably high stability. The embedment C-PSCs were mainly prepared and investigated by Yang's group,[31,37,38,44,59] which indicated that these devices could retain its performance after storage in dark conditions for tens of days. Very recently, results on the embedment C-PSCs based on B-doped multi wall carbon nanotubes indicated that these devices not only could get a high PCE of 15.23% but also exhibited a considerably high stability, which could retain their performance at room temperature in air for 80 days and at 80 °C for 14 days.[44]

Since the carbon electrode in paintable C-PSCs is composed of carbon materials and polymer additives, the wettability of the carbon electrode is reduced [Fig. 3(a)], which could smoothen the serious attack from surrounding water molecules. Therefore, the paintable C-PSCs usually exhibited a high stability in ambient conditions or even under water.[32,34,40] For example, a custom carbon paint developed by Zhou et al. resulted in a no PCE decay of a nonencapsulated device after 2446 h.[40] Besides, Wei et al. demonstrated that the carbon electrodes with epoxy well improved the performance stability under water immersion, and after further forming a hydrophobic Ag coating from Ag paint, the performance could retain most of the initial PCE for over 1 h.[34] Furthermore, Yu et al. demonstrated that about 98 and 92% of the initial PCE of their devices were retained after exposing the paintable C-PSCs to water flushing [Figs. 3(c) and 3(d)], respectively.[60] Though many reported paintable C-PSCs have shown excellent stability, stability testing under more practical conditions, such as light soaking conditions, high temperature (e.g., 80 °C), etc., is still lacking.

IV. SCALING UP OF C-PSCS

Since C-PSCs have demonstrated considerably high stability together with decent PCEs, some groups and companies are considering scaling up the device production. However, conventional spin coating technique was only suitable for small-area devices, which could not be simply scaled up. The special architecture and fabrication process of meso C-PSCs facilitates the use of scalable screen-printing technique for automated production. The most recent demonstrated meso C-PSCs were illustrated in Fig. 4(a), in which batch processing on rigid glass substrates was realized by screen-printing techniques [shown in Fig. 4(b)].[53,61] The final solar cell module was exhibited in Fig. 4(c), which has achieved a PCE over 10% for large active areas of 70 and 49 cm^2 (Table II).[53,61] Hu et al. have made a more forward step to enlarge the module area to 7 m^2, which could be directly used to power a panel.[53] All these achievements have implied the nearest term for PSCs commercialization. For practical application, auto production line needs to be developed for enabling continuous and controllable

TABLE I. Representative stability testing data reported of C-PSCs and HTM-PSCs.

PSCs	Structures	Encapsulation	Light soaking	Thermal	Duration (h)	Outdoor	Notes	Ref.
C-PSCs	$TiO_2/ZrO_2/(5\text{-AVA})_x(MA)_{1-x}PbI_3/C$	No	AM1.5 G, 100 mW/cm^2	RT	1000	No	...	30
	$TiO_2/ZrO_2/(5\text{-AVA})_x(MA)_{1-x}PbI_3/C$	Yes	Dark Natural light	85 °C Ambient	2160 168	No Jeddah	...	51
	$TiO_2/ZrO_2/MAPbI_3/C$	Yes	Dark	100 °C	1500	No	...	52
	NiMgLiO/$MAPbI_3$/PCBM/Ti(Nb)O_x/Ag	Yes	AM1.5 G, 100 mW/cm^2	RT	1000	No	UV light is filtered	50
	PEDOT:PSS/$(BA)_2(MA)_3Pb_4I_{13}$/PCBM/Al	Yes	AM1.5 G, 100 mW/cm^2	RT	2750	No	2D PVK, PCE = 12.52%	57
HTM-PSCs	$TiO_2/Rb_{0.05}(Cs_{0.05}(MA_{0.17}FA_{0.83})_{0.95})_{0.95}(I_{0.83}Br_{0.17})_3$/Spiro/Au	Yes	AM1.5 G, 100 mW/cm^2	85 °C	500	No	N_2 atmosphere	56
	$TiO_2/FA_{0.83}MA_{0.17}PbI_{2.5}Br_{0.5}$/Spiro/Au	Yes	Natural light	Ambient	2160	Turin	UV light is filtered	54
	FTO/LBSO/$MAPbI_3$/NiO/FTO	Yes	AM1.5 G, 100 mW/cm^2	RT	1000	No	All inorganic collection layer, PCE = 14.4%	58
	$TiO_2/Cs_{0.05}FA_{0.81}MA_{0.14}PbI_{2.55}Br_{0.45}$/Spiro/Au	Yes	AM1.5 G, 100 mW/cm^2	RT	500	No	N_2 atmosphere, UV light is filtered	55

https://doi.org/10.1557/jmr.2017.294 Published online by Cambridge University Press

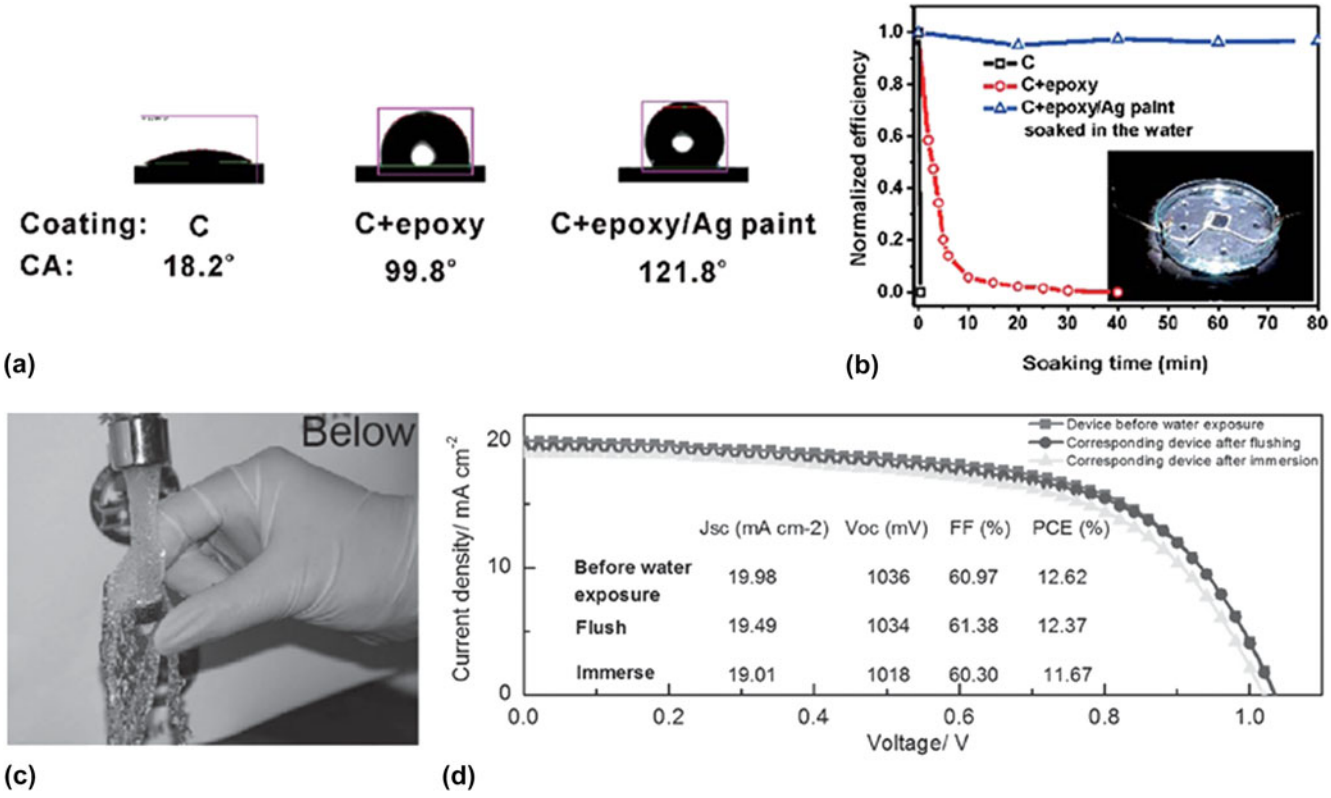


FIG. 3. Stability of C-PSCs under water. (a) Contact angle photographs of three electrodes: pure carbon, carbon/epoxy, and carbon/epoxy/Ag paint and (b) Normalized efficiency as a function of soaking time in water (measured by recording *J–V* curves of the PSCs immersed in water). Reprinted with permission from Ref. 34. Copyright 2015, Royal Chemical Society. The inset shows the measurement setup. (c) Photograph of the as-prepared PSCs placed under running water, and (d) *J–V* curves of the as-prepared C-PSCs before and after water exposure. Reprinted with permission from Ref. 60. Copyright 2016, Wiley.

fabrication process of the module. The proposed production line has also been given by Hu et al. in Fig. 4(d).[53] As indicated, the conduction glasses were first etched by laser, followed by the sequential deposition of compact TiO_2, mesoporous TiO_2, mesoporous ZrO_2, and mesoporous carbon layers by screen printing. Finally, perovskite solution could be deposited by screen printing, doctor blade, or inkjet printing technique.

Several other techniques have also been exploited for large-scale fabrication of C-PSCs. For the large-scale deposition of carbon electrodes, Wei et al. have exploited inkjet printing techniques to deposit carbon electrodes in embedment C-PSCs.[31] Two strategies have been designed to realize the idea. The first one is that carbon could be directly deposited on the PbI_2 layer, followed by postconversion to perovskite. The other one is ingenious, in which carbon/MAI ink was developed. During inkjet printing, carbon electrodes and chemical conversions happened simultaneously, which obviated the predeposition process of carbon electrodes.[31] The application of inkjet printing makes the deposition of carbon electrodes scalable and controllable. Besides, this strategy resulted in an interpenetrating interface between $MAPbI_3$ and carbon electrodes for deducing charge recombination and increasing PCE. As reported afterward, perovskite layer could also be deposited by inkjet printing,[62] which further made the inkjet printing technique more promising for scaling up the C-PSCs.

For the production of C-PSCs or PSCs, the processes developed for OPVs could also be adaptable. As a compatible technique with a roll-to-roll, slot-die coating technology, that is, a noncontact large-area fabrication technique has achieved success in large-scale OPVs fabrication. As a result, slot-die coating technology has been also exploited to deposit perovskite layer in PSCs.[63] Recently, Weihua-Solar Company used a slot-die coating technology to produce large-scale perovskite layers for paintable C-PSCs ($ZnO/MAPbI_3/C$) panels as shown in Fig. 5(b), which could be easily scaled up (such as 45 × 65 cm).[12] The 25 cm^2 modules achieved a promising PCE of 10.6% with a negligible degradation after 140 days of outdoor testing.[64]

Besides, Chen et al. have developed a mature electrodeposition strategy to deposit the PbI_2 precursor on TiO_2 scaffold,[33] as shown in Fig. 5(c). Firstly, electrodeposition technique was applied to deposit PbO_2. Then, PbO_2 was converted to PbI_2 by the immersion in HI ethanol solution. Finally, PbI_2 was converted to dark brown

https://doi.org/10.1557/jmr.2017.294 Published online by Cambridge University Press

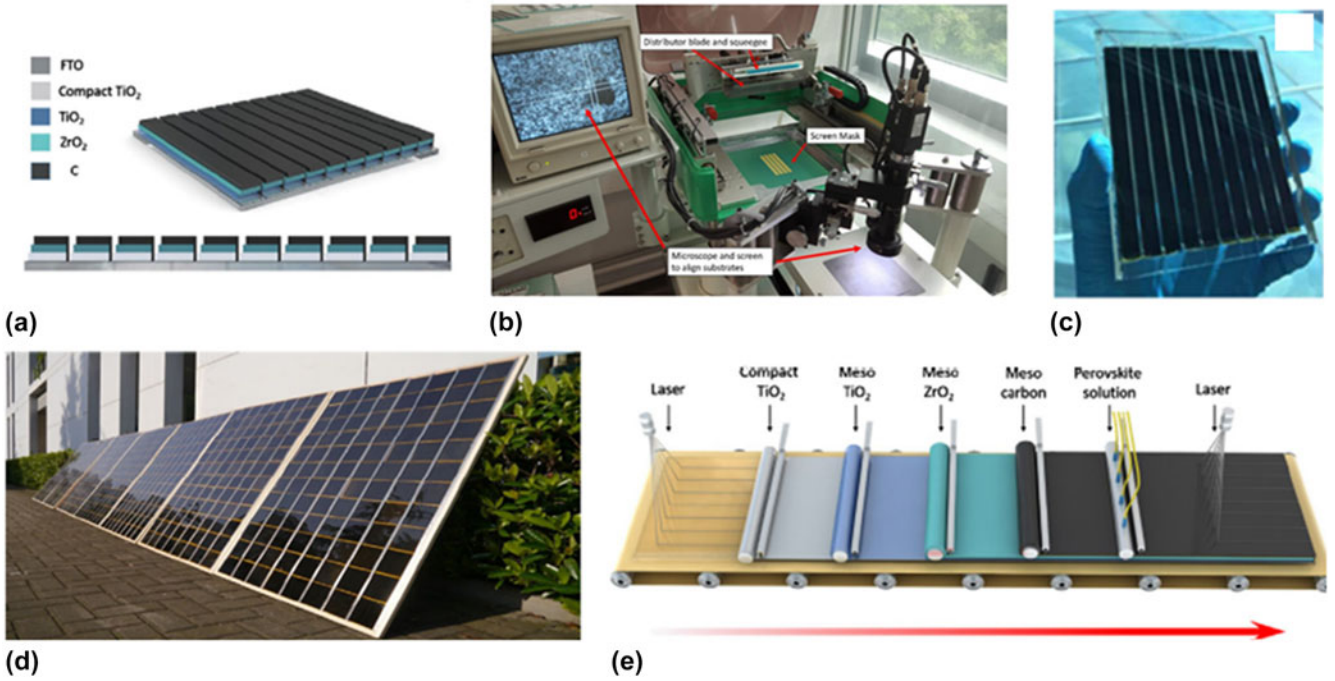


FIG. 4. Fabrication of large-scale meso C-PSCs. (a) Structure scheme of solar module. Reprinted with permission from Ref. 53. Copyright 2017, Wiley. (b) Photograph of semi-automatic screen printer and (c) meso C-PSCs module prepared by screen printer. Reprinted with permission from Ref. 61. Copyright 2016, Royal Chemical Society. (d) Solar panel of meso C-PSCs, and (e) schematic illustration of the proposed production line of meso C-PSCs. Reprinted with permission from Ref. 53. Copyright 2017, Wiley.

TABLE II. Reported data for large-scale C-PSCs.

Structure	Type of C-PSCs	Technique	Area (cm^2)	PCE (%)	Ref.
$TiO_2/ZrO_2/(5\text{-}AVA)_x(MA)_{1-x}PbI_3/C$	Meso C-PSCs	Screen printing	70	10.74	61
$TiO_2/ZrO_2/(5\text{-}AVA)_x(MA)_{1-x}PbI_3/C$	Meso C-PSCs	Screen printing	49	10.40	53
$TiO_2/MAPbI_3/C$	Paintable C-PSCs	Electrodeposition	4	4.47	33
$ZnO/MAPbI_3/C$	Paintable C-PSCs	Slot-die coating	25	10.60	64

colored $MAPbI_3$ in MAI solution. This whole low-temperature electrodeposition procedure was obviously scalable in substrate size, as shown in Fig. 5(d). In addition, this technique was flexible for a variety of disparate substrate shapes and forms and was roll-to-roll compatible. In combination with the painting process for carbon electrode deposition, the paintable C-PSCs could be easily scaled up. The large-scale paintable C-PSCs (4 cm^2) fabricated by these electrodepositions and painting techniques achieved a promising PCE of 4.47% (Table II).

V. PENDING ISSUES AND FUTURE RESEARCH DIRECTIONS

In spite of the obviously higher stability of C-PSCs than HTM-PSCs, the stability of C-PSCs is still significantly lower than that of silicon and thin film solar cells, which calls for more efforts to further improve the stability before their commercialization. So far, more works on C-PSCs are based on $MAPbI_3$ perovskites, whose stability is not high. To further improve the stability of C-PSCs, new and more stable mixed perovskites should be exploited, such as $FA_{0.81}MA_{0.15}PbI_{2.55}Br_{0.45}$,[2] $Cs_{0.05}FA_{0.81}MA_{0.14}PbI_{2.55}Br_{0.45}$,[54] $Rb_{0.05}(Cs_{0.05}(MA_{0.17}FA_{0.83})_{0.95})_{0.95}(I_{0.83}Br_{0.17})_3$,[56] and so on. Since ultraviolet (UV) light would induce severe degradation of perovskites, the application of UV light filter coating may be a promising approach. For example, by coating a luminescent photopolymer layer on the front side of an FTO glass, UV light was absorbed to re-emit in the visible range to both increase photocurrent and avoid UV-induced degradation.[54] Besides, to increase the humidity resistance of C-PSCs, the modification of the carbon electrode with superhydrophobic molecules could be another choice to enhance the device stability.

Though some scaling-up techniques have been developed to prepare a large-area perovskite layer for

https://doi.org/10.1557/jmr.2017.294 Published online by Cambridge University Press

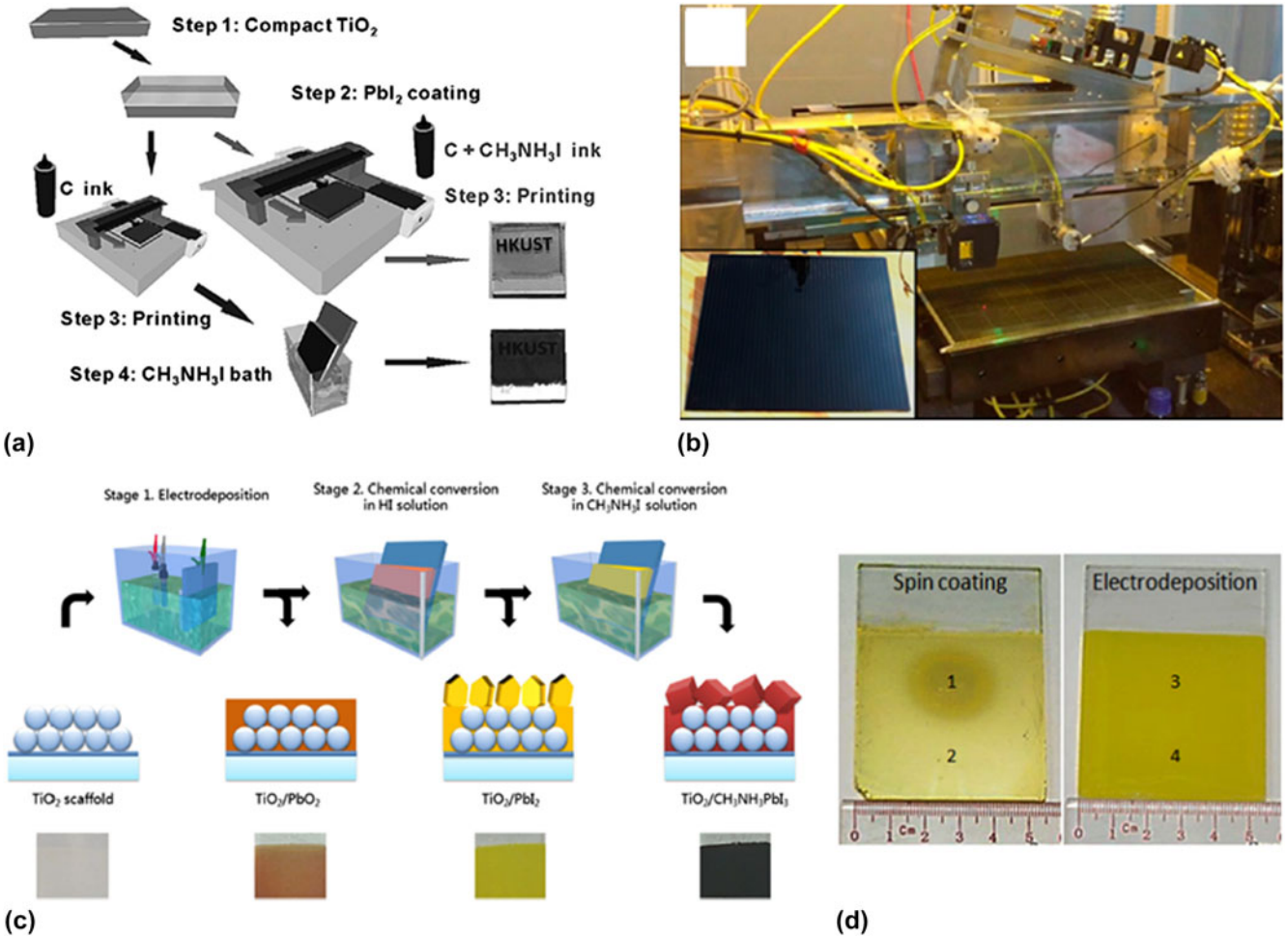


FIG. 5. Some reported scaling-up techniques for the fabrication of C-PSCs. (a) Inkjet printing. Reprinted with permission from Ref. 31. Copyright 2014, Wiley. (b) Slot-die coating technology. Reprinted with permission from Ref. 12. Copyright 2016, American Chemical Society. (c) Electrodeposition, and (d) photographs of the large-scale PbI_2 precursors prepared by spin coating and electrodeposition. Reprinted with permission from Ref. 33. Copyright 2015, Elsevier.

C-PSCs, the challenge remains to be able to consistently form a uniform, high-purity perovskite layer at large scale due to the difficulty in controlling crystallization behavior, which still significantly limits the PCE of C-PSCs modules. Therefore, the future development and optimization of large-scale deposition technologies is needed to accelerate the commercialization of C-PSCs. In fact, some successful researches on post treatment seem to have spotted a light on solving this issue. Typically, MA gas treatment on the predeposited $MAPbI_3$ layer has been proved to considerably improve the film morphology and crystal quality,[65] which is attributed to the formation of high-liquidity $MAPbI_3{\cdot}x$MA intermediate phase for inducing a reconstruction to get a smooth and uniform film.[65,66] Besides, NH_3,[67] DMF,[68] and DMSO,[69] gas treatment has also shown a positive effect on improving the morphology and crystal quality of the perovskite layer, which may be exploited to increase the quality of the large-scale perovskite layer. In addition, the series resistance of the FTO glass and carbon electrode should be reduced to improve the FF and PCE of large-area C-PSCs.

VI. CONCLUSIONS

We have summarized the recent progresses on the device stability and the scaling up of C-PSCs. The different types of C-PSCs, including meso C-PSCs, embedment C-PSCs, and paintable C-PSCs have exhibited significantly high stability, which is still being improved steadily. In addition, due to the high water resistance property of the carbon electrode, some C-PSCs could even work well under water immersion or water flushing. Since the mesoporous layers in meso PSCs could be deposited by scalable screen-printing techniques, the large-scale meso C-PSCs with high performance have been well fabricated and reported. In addition to screen printing, other promising scalable

https://doi.org/10.1557/jmr.2017.294 Published online by Cambridge University Press

techniques, including inkjet printing, slot-die coating, and electrodeposition have also been exploited for the large-scale fabrication of C-PSCs. Though great progresses have been achieved, some issues on device stability and scaling-up production still need to be addressed to further promote the commercialization of C-PSCs.

ACKNOWLEDGMENTS

This work is financially supported by the Young Talent of "Zhuoyue" Program of Beihang University, the National Natural Science Foundation of China (Nos. 51371020 and 21603010), the HK-RGC General Research Funds (GRF Nos. 16312216 and 16300915), and the HK Innovation and Technology Fund (ITS/219/16).

REFERENCES

1. NREL: (2017). Available at: https://www.nrel.gov/pv/assets/images/efficiency-chart.png (accessed July, 2017).
2. X. Li, D. Bi, C. Yi, J.D. Decoppet, J. Luo, S.M. Zakeeruddin, A. Hagfeldt, and M. Gratzel: A vacuum flash-assisted solution process for high-efficiency large-area perovskite solar cells. *Science* **353**, 58 (2016).
3. A. Kojima, K. Teshima, Y. Shirai, and T. Miyasaka: Organometal halide perovskites as visible-light sensitizers for photovoltaic cells. *J. Am. Chem. Soc.* **131**, 6050 (2009).
4. W.S. Yang, J.H. Noh, N.J. Jeon, Y.C. Kim, S. Ryu, J. Seo, and S.I. Seok: Solar cells high-performance photovoltaic perovskite layers fabricated through intramolecular exchange. *Science* **348**, 1234 (2015).
5. Y. Bai, H.N. Chen, S. Xiao, Q.F. Xue, T. Zhang, Z.L. Zhu, Q. Li, C. Hu, Y. Yang, Z.C. Hu, F. Huang, K.S. Wong, H.L. Yip, and S.H. Yang: Effects of a molecular monolayer modification of NiO nanocrystal layer surfaces on perovskite crystallization and interface contact toward faster hole extraction and higher photovoltaic performance. *Adv. Funct. Mater.* **26**, 2950 (2016).
6. K. Yan, M. Long, T. Zhang, Z. Wei, H. Chen, S. Yang, and J. Xu: Hybrid halide perovskite solar cell precursors: Colloidal chemistry and coordination engineering behind device processing for high efficiency. *J. Am. Chem. Soc.* **137**, 4460 (2015).
7. J.H. Im, I.H. Jang, N. Pellet, M. Gratzel, and N.G. Park: Growth of $CH_3NH_3PbI_3$ cuboids with controlled size for high-efficiency perovskite solar cells. *Nat. Nanotechnol.* **9**, 927 (2014).
8. N.J. Jeon, J.H. Noh, Y.C. Kim, W.S. Yang, S. Ryu, and S.I. Seok: Solvent engineering for high-performance inorganic–organic hybrid perovskite solar cells. *Nat. Mater.* **13**, 897 (2014).
9. T. Zhang, H. Chen, Y. Bai, S. Xiao, L. Zhu, C. Hu, Q. Xue, and S. Yang: Understanding the relationship between ion migration and the anomalous hysteresis in high-efficiency perovskite solar cells: A fresh perspective from halide substitution. *Nano Energy* **26**, 620 (2016).
10. D. Bi, W. Tress, M.I. Dar, P. Gao, J. Luo, C. Renevier, K. Schenk, A. Abate, F. Giordano, J.P. Correa Baena, J.D. Decoppet, S.M. Zakeeruddin, M.K. Nazeeruddin, M. Gratzel, and A. Hagfeldt: Efficient luminescent solar cells based on tailored mixed-cation perovskites. *Sci. Adv.* **2**, e1501170 (2016).
11. D. Bi, C. Yi, J. Luo, J-D. Décoppet, F. Zhang, S.M. Zakeeruddin, X. Li, A. Hagfeldt, and M. Grätzel: Polymer-templated nucleation and crystal growth of perovskite films for solar cells with efficiency greater than 21%. *Nat. Energy* **1**, 16142 (2016).
12. Y. Zhou and K. Zhu: Perovskite solar cells shine in the "valley of the sun". *ACS Energy Lett.* **1**(1), 64 (2016).
13. S.Y. Sun, T. Salim, N. Mathews, M. Duchamp, C. Boothroyd, G.C. Xing, T.C. Sum, and Y.M. Lam: The origin of high efficiency in low-temperature solution-processable bilayer organometal halide hybrid solar cells. *Energy Environ. Sci.* **7**, 399 (2014).
14. C.S. Ponseca, Jr., T.J. Savenije, M. Abdellah, K. Zheng, A. Yartsev, T. Pascher, T. Harlang, P. Chabera, T. Pullerits, A. Stepanov, J.P. Wolf, and V. Sundstrom: Organometal halide perovskite solar cell materials rationalized: Ultrafast charge generation, high and microsecond-long balanced mobilities, and slow recombination. *J. Am. Chem. Soc.* **136**, 5189 (2014).
15. Q. Dong, Y. Fang, Y. Shao, P. Mulligan, J. Qiu, L. Cao, and J. Huang: Electron-hole diffusion lengths >175 mum in solution-grown $CH_3NH_3PbI_3$ single crystals. *Science* **347**, 967 (2015).
16. D. Shi, V. Adinolfi, R. Comin, M. Yuan, E. Alarousu, A. Buin, Y. Chen, S. Hoogland, A. Rothenberger, K. Katsiev, Y. Losovyj, X. Zhang, P.A. Dowben, O.F. Mohammed, E.H. Sargent, and O.M. Bakr: Low trap-state density and long carrier diffusion in organolead trihalide perovskite single crystals. *Science* **347**, 519 (2015).
17. K-G. Lim, S. Ahn, Y-H. Kim, Y. Qi, and T-W. Lee: Universal energy level tailoring of self-organized hole extraction layers in organic solar cells and organic–inorganic hybrid perovskite solar cells. *Energy Environ. Sci.* **9**, 932 (2016).
18. S.D. Stranks, G.E. Eperon, G. Grancini, C. Menelaou, M.J. Alcocer, T. Leijtens, L.M. Herz, A. Petrozza, and H.J. Snaith: Electron-hole diffusion lengths exceeding 1 micrometer in an organometal trihalide perovskite absorber. *Science* **342**, 341 (2013).
19. G. Xing, N. Mathews, S. Sun, S.S. Lim, Y.M. Lam, M. Gratzel, S. Mhaisalkar, and T.C. Sum: Long-range balanced electron- and hole-transport lengths in organic–inorganic $CH_3NH_3PbI_3$. *Science* **342**, 344 (2013).
20. V. D'Innocenzo, G. Grancini, M.J. Alcocer, A.R. Kandada, S.D. Stranks, M.M. Lee, G. Lanzani, H.J. Snaith, and A. Petrozza: Excitons versus free charges in organo-lead tri-halide perovskites. *Nat. Commun.* **5**, 3586 (2014).
21. T.A. Berhe, W.N. Su, C.H. Chen, C.J. Pan, J.H. Cheng, H.M. Chen, M.C. Tsai, L.Y. Chen, A.A. Dubale, and B.J. Hwang: Organometal halide perovskite solar cells: Degradation and stability. *Energy Environ. Sci.* **9**, 323 (2016).
22. P. Docampo and T. Bein: A long-term view on perovskite optoelectronics. *Acc. Chem. Res.* **49**, 339 (2016).
23. M. Shahbazi and H. Wang: Progress in research on the stability of organometal perovskite solar cells. *J. Sol. Energy* **123**, 74 (2016).
24. D. Wang, M. Wright, N.K. Elumalai, and A. Uddin: Stability of perovskite solar cells. *Sol. Energy Mater. Sol. Cells* **147**, 255 (2016).
25. M.D. Ye, X.D. Hong, F.Y. Zhang, and X.Y. Liu: Recent advancements in perovskite solar cells: Flexibility, stability and large scale. *J. Mater. Chem. A* **4**, 6755 (2016).
26. H. Back, G. Kim, J. Kim, J. Kong, T.K. Kim, H. Kang, H. Kim, J. Lee, S. Lee, and K. Lee: Achieving long-term stable perovskite solar cells via ion neutralization. *Energy Environ. Sci.* **9**, 1258 (2016).
27. K. Domanski, J-P. Correa-Baena, N. Mine, M.K. Nazeeruddin, A. Abate, M. Saliba, W. Tress, A. Hagfeldt, and M. Grätzel: Not all that glitters is gold: Metal migration-induced degradation in perovskite solar cells. *ACS Nano* **10**, 6306 (2016).
28. L. Etgar, P. Gao, Z. Xue, Q. Peng, A.K. Chandiran, B. Liu, M.K. Nazeeruddin, and M. Gratzel: Mesoscopic $CH_3NH_3PbI_3$/TiO_2 heterojunction solar cells. *J. Am. Chem. Soc.* **134**, 17396 (2012).

https://doi.org/10.1557/jmr.2017.294 Published online by Cambridge University Press

29. Z. Ku, Y. Rong, M. Xu, T. Liu, and H. Han: Full printable processed mesoscopic $CH_3NH_3PbI_3/TiO_2$ heterojunction solar cells with carbon counter electrode. *Sci. Rep.* **3**, 3132 (2013).
30. A. Mei, X. Li, L. Liu, Z. Ku, T. Liu, Y. Rong, M. Xu, M. Hu, J. Chen, Y. Yang, M. Gratzel, and H. Han: A hole-conductor-free, fully printable mesoscopic perovskite solar cell with high stability. *Science* **345**, 295 (2014).
31. Z. Wei, H. Chen, K. Yan, and S. Yang: Inkjet printing and instant chemical transformation of a $CH_3NH_3PbI_3$/nanocarbon electrode and interface for planar perovskite solar cells. *Angew. Chem.* **53**, 13239 (2014).
32. F. Zhang, X. Yang, H. Wang, M. Cheng, J. Zhao, and L. Sun: Structure engineering of hole-conductor free perovskite-based solar cells with low-temperature-processed commercial carbon paste as cathode. *ACS Appl. Mater. Interfaces* **6**, 16140 (2014).
33. H.N. Chen, Z.H. Wei, X.L. Zheng, and S.H. Yang: A scalable electrodeposition route to the low-cost, versatile and controllable fabrication of perovskite solar cells. *Nano Energy* **15**, 216 (2015).
34. Z.H. Wei, X.L. Zheng, H.N. Chen, X. Long, Z.L. Wang, and S.H. Yang: A multifunctional C plus epoxy/Ag-paint cathode enables efficient and stable operation of perovskite solar cells in watery environments. *J. Mater. Chem. A* **3**, 16430 (2015).
35. W.A. Laban and L. Etgar: Depleted hole conductor-free lead halide iodide heterojunction solar cells. *Energy Environ. Sci.* **6**, 3249 (2013).
36. Z. Ku, X. Xia, H. Shen, N.H. Tiep, and H.J. Fan: A mesoporous nickel counter electrode for printable and reusable perovskite solar cells. *Nanoscale* **7**, 13363 (2015).
37. Z.H. Wei, K.Y. Yan, H.N. Chen, Y. Yi, T. Zhang, X. Long, J.K. Li, L.X. Zhang, J.N. Wang, and S.H. Yang: Cost-efficient clamping solar cells using candle soot for hole extraction from ambipolar perovskites. *Energy Environ. Sci.* **7**, 3326 (2014).
38. H. Chen, Z. Wei, K. Yan, Y. Yi, J. Wang, and S. Yang: Liquid phase deposition of TiO_2 nanolayer affords $CH_3NH_3PbI_3$/nanocarbon solar cells with high open-circuit voltage. *Faraday Discuss.* **176**, 271 (2014).
39. H. Chen and S. Yang: High-quality perovskite in thick scaffold: A core issue for hole transport material-free perovskite solar cells. *Sci. Bull.* **61**, 1680 (2016).
40. H. Zhou, Y. Shi, Q. Dong, H. Zhang, Y. Xing, K. Wang, Y. Du, and T. Ma: Hole-conductor-free, metal-electrode-free TiO_2/$CH_3NH_3PbI_3$ heterojunction solar cells based on a low-temperature carbon electrode. *J. Phys. Chem. Lett.* **5**, 3241 (2014).
41. H. Chen and S. Yang: Carbon-based perovskite solar cells without hole transport materials: The front runner to the market? *Adv. Mater.* **29**, 1603994 (2017).
42. Y. Rong, X. Hou, Y. Hu, A. Mei, L. Liu, P. Wang, and H. Han: Synergy of ammonium chloride and moisture on perovskite crystallization for efficient printable mesoscopic solar cells. *Nat. Commun.* **8**, 14555 (2017).
43. H. Zhang, H. Wang, S.T. Williams, D. Xiong, W. Zhang, C-C. Chueh, W. Chen, and A.K.Y. Jen: $SrCl_2$ derived perovskite facilitating a high efficiency of 16% in hole-conductor-free fully printable mesoscopic perovskite solar cells. *Adv. Mater.* **29**, 1606608 (2017).
44. X. Zheng, H. Chen, Q. Li, Y. Yang, Z. Wei, Y. Bai, Y. Qiu, D. Zhou, K.S. Wong, and S. Yang: Boron doping of multiwalled carbon nanotubes significantly enhances hole extraction in carbon-based perovskite solar cells. *Nano Lett.* **17**, 2496 (2017).
45. H. Chen, X. Zheng, Q. Li, Y. Yang, S. Xiao, C. Hu, Y. Bai, T. Zhang, K.S. Wong, and S. Yang: An amorphous precursor route to the conformable oriented crystallization of $CH_3NH_3PbBr_3$ in mesoporous scaffolds: Toward efficient and thermally stable carbon-based perovskite solar cells. *J. Mater. Chem. A* **4**, 12897 (2016).
46. H.N. Chen, Z.H. Wei, H.X. He, X.L. Zheng, K.S. Wong, and S.H. Yang: Solvent engineering boosts the efficiency of paintable carbon-based perovskite solar cells to beyond 14%. *Adv. Energy Mater.* **6**, 1502087 (2016).
47. X. Chang, W. Li, H. Chen, L. Zhu, H. Liu, H. Geng, S. Xiang, J. Liu, X. Zheng, Y. Yang, and S. Yang: Colloidal precursor-induced growth of ultra-even $CH_3NH_3PbI_3$ for high-performance paintable carbon-based perovskite solar cells. *ACS Appl. Mater. Interfaces* **8**, 30184 (2016).
48. Y. Sheng, Y. Hu, A. Mei, P. Jiang, X. Hou, M. Duan, L. Hong, Y. Guan, Y. Rong, Y. Xiong, and H. Han: Enhanced electronic properties in $CH_3NH_3PbI_3$ via LiCl mixing for hole-conductor-free printable perovskite solar cells. *J. Mater. Chem. A* **4**, 16731 (2016).
49. C.Y. Chan, Y.Y. Wang, G.W. Wu, and E.W.G. Diau: Solvent-extraction crystal growth for highly efficient carbon-based mesoscopic perovskite solar cells free of hole conductors. *J. Mater. Chem. A* **4**, 3872 (2016).
50. W. Chen, Y. Wu, Y. Yue, J. Liu, W. Zhang, X. Yang, H. Chen, E. Bi, I. Ashraful, M. Gratzel, and L. Han: Efficient and stable large-area perovskite solar cells with inorganic charge extraction layers. *Science* **350**, 944 (2015).
51. X. Li, M. Tschumi, H.W. Han, S.S. Babkair, R.A. Alzubaydi, A.A. Ansari, S.S. Habib, M.K. Nazeeruddin, S.M. Zakeeruddin, and M. Gratzel: Outdoor performance and stability under elevated temperatures and long-term light soaking of triple-layer mesoporous perovskite photovoltaics. *Energy Technol.* **3**, 551 (2015).
52. A.K. Baranwal, S. Kanaya, T.A.N. Peiris, G. Mizuta, T. Nishina, H. Kanda, T. Miyasaka, H. Segawa, and S. Ito: 100 °C thermal stability of printable perovskite solar cells using porous carbon counter electrodes. *ChemSusChem* **9**, 2517 (2016).
53. Y. Hu, S. Si, A. Mei, Y. Rong, H. Liu, X. Li, and H. Han: Stable large-area (10×10 cm^2) printable mesoscopic perovskite module exceeding 10% efficiency. *Sol. RRL* **1**, 1600019 (2017).
54. F. Bella, G. Griffini, J-P. Correa-Baena, G. Saracco, M. Grätzel, A. Hagfeldt, S. Turri, and C. Gerbaldi: Improving efficiency and stability of perovskite solar cells with photocurable fluoropolymers. *Science* **354**, 203 (2016).
55. H. Tan, A. Jain, O. Voznyy, X. Lan, F.P. Garcia de Arquer, J.Z. Fan, R. Quintero-Bermudez, M. Yuan, B. Zhang, Y. Zhao, F. Fan, P. Li, L.N. Quan, Y. Zhao, Z.H. Lu, Z. Yang, S. Hoogland, and E.H. Sargent: Efficient and stable solution-processed planar perovskite solar cells via contact passivation. *Science* **355**, 722 (2017).
56. M. Saliba, T. Matsui, K. Domanski, J.Y. Seo, A. Ummadisingu, S.M. Zakeeruddin, J.P. Correa-Baena, W.R. Tress, A. Abate, A. Hagfeldt, and M. Gratzel: Incorporation of rubidium cations into perovskite solar cells improves photovoltaic performance. *Science* **354**, 206 (2016).
57. H. Tsai, W. Nie, J-C. Blancon, C.C. Stoumpos, R. Asadpour, B. Harutyunyan, A.J. Neukirch, R. Verduzco, J.J. Crochet, S. Tretiak, L. Pedesseau, J. Even, M.A. Alam, G. Gupta, J. Lou, P.M. Ajayan, M.J. Bedzyk, M.G. Kanatzidis, and A.D. Mohite: High-efficiency two-dimensional Ruddlesden–Popper perovskite solar cells. *Nature* **536**, 312 (2016).
58. S.S. Shin, E.J. Yeom, W.S. Yang, S. Hur, M.G. Kim, J. Im, J. Seo, J.H. Noh, and S.I. Seok: Colloidally prepared La-doped $BaSnO_3$ electrodes for efficient, photostable perovskite solar cells. *Science* **356**, 167 (2017).
59. Z.H. Wei, H.N. Chen, K.Y. Yan, X.L. Zheng, and S.H. Yang: Hysteresis-free multi-walled carbon nanotube-based perovskite solar cells with a high fill factor. *J. Mater. Chem. A* **3**, 24226 (2015).
60. Z.H. Yu, B.L. Chen, P. Liu, C.L. Wang, C.H. Bu, N.A. Cheng, S.H. Bai, Y.F. Yan, and X.Z. Zhao: Stable organic–inorganic

https://doi.org/10.1557/jmr.2017.294 Published online by Cambridge University Press

perovskite solar cells without hole-conductor layer achieved via cell structure design and contact engineering. *Adv. Funct. Mater.* **26**, 4866 (2016).
61. A. Priyadarshi, L.J. Haur, P. Murray, D. Fu, S. Kulkarni, G. Xing, T.C. Sum, N. Mathews, and S.G. Mhaisalkar: A large area (70 cm^2) monolithic perovskite solar module with a high efficiency and stability. *Energy Environ. Sci.* **9**, 3687 (2016).
62. S-G. Li, K-J. Jiang, M-J. Su, X-P. Cui, J-H. Huang, Q-Q. Zhang, X-Q. Zhou, L-M. Yang, and Y-L. Song: Inkjet printing of $CH_3NH_3PbI_3$ on a mesoscopic TiO_2 film for highly efficient perovskite solar cells. *J. Mater. Chem. A* **3**, 9092 (2015).
63. K. Hwang, Y-S. Jung, Y-J. Heo, F.H. Scholes, S.E. Watkins, J. Subbiah, D.J. Jones, D-Y. Kim, and D. Vak: Toward large scale roll-to-roll production of fully printed perovskite solar cells. *Adv. Mater.* **27**, 1241 (2015).
64. C. Longhua, L. Lusheng, W. Jifeng, D. Bin, G. Lili, and F. Bin: Large area perovskite solar cell module. *J. Semicond.* **38**, 014006 (2017).
65. Z. Zhou, Z. Wang, Y. Zhou, S. Pang, D. Wang, H. Xu, Z. Liu, N.P. Padture, and G. Cui: Methylamine-gas-induced defect-healing behavior of $CH_3NH_3PbI_3$ thin films for perovskite solar cells. *Angew. Chem.* **127**, 9841 (2015).
66. S. Pang, Y. Zhou, Z. Wang, M. Yang, A.R. Krause, Z. Zhou, K. Zhu, N.P. Padture, and G. Cui: Transformative evolution of organolead triiodide perovskite thin films from strong room-temperature solid-gas interaction between $HPbI_3$–CH_3NH_2 precursor pair. *J. Am. Chem. Soc.* **138**, 750 (2016).
67. Y. Zhao and K. Zhu: Optical bleaching of perovskite $(CH_3NH_3)PbI_3$ through room-temperature phase transformation induced by ammonia. *Chem. Commun.* **50**, 1605 (2014).
68. Z. Xiao, Q. Dong, C. Bi, Y. Shao, Y. Yuan, and J. Huang: Solvent annealing of perovskite-induced crystal growth for photovoltaic-device efficiency enhancement. *Adv. Mater.* **26**, 6503 (2014).
69. Y. Wu, W. Chen, Y. Yue, J. Liu, E. Bi, X. Yang, A. Islam, and L. Han: Consecutive morphology controlling operations for highly reproducible mesostructured perovskite solar cells. *ACS Appl. Mater. Interfaces* **7**, 20707 (2015).

https://doi.org/10.1557/jmr.2017.294 Published online by Cambridge University Press